J Mater Sci (2011) 46:4906–4912
DOI 10.1007/s10853-011-5403-1

Hydrothermal synthesis of ultra-thin $LiFePO_4$ platelets for Li-ion batteries

Hongfa Xiang · Dawei Zhang · Yi Jin · Chunhua Chen · Jishan Wu · Haihui Wang

Received: 10 December 2010 / Accepted: 15 February 2011 / Published online: 24 February 2011

Abstract Ultra-thin $LiFePO_4$ platelets are prepared by a hydrothermal process using tetraethylene glycol as co-solvent. The prepared $LiFePO_4$ platelets have a very thin thickness of about 50–80 nm, which is beneficial for Li ions to fast transfer in the bulk of the electrode. It is found that the as-synthesized $LiFePO_4$ cathode material exhibits a quite high reversible capacity of 137 mAh g^{-1} at 0.2 C. After carbon coating, the obtained $LiFePO_4$/C composite cathode has the enhanced electronic conductivity, and thus the rate capability has been improved significantly. At 8 and 12 C, the composite has the discharge capacity of 104 and 95 mAh g^{-1}, respectively, which suggests that the ultra-thin $LiFePO_4$ platelets are a promising candidate for the large-scale Li-ion batteries.

Introduction

After the successful application and great development of lithium-ion batteries in the portable electronic devices, now the large-scale Li-ion batteries are growing in popularity for use in electric vehicles (EV) field and the energy storage for the renewable energy, i.e., wind and solar energies, owing to their high energy density [1, 2]. However, to meet the requirement for the wider application and development of the large-scale Li-ion batteries, the safety characteristic and lifespan of the state-of-the-art Li-ion batteries should be improved further [3]. $LiFePO_4$ is one of the most promising cathode materials for the next-generation Li-ion batteries with better safety characteristic and longer lifespan.

$LiFePO_4$ has been particularly attractive to the present battery industry due to its low cost, environmental benignancy and excellent safety characteristic, as well as high theoretical capacity (170 mAh g^{-1}), flat voltage plateau ($\sim$3.45 V vs. Li^+/Li) and excellent cycling performance [4, 5]. However, its poor conductivity both for electron and ion transfer is one of the main obstacles for its wide commercial application [6, 7]. In order to improve the electronic conductivity of $LiFePO_4$, coating an electronically conductive phase (typically carbon, metals, or conductive polymers, etc.) is an effective way [8–12]. Minimizing the particle size and doping with foreign atoms are frequently validated to be convenient to overcome the limitation of ion transfer [13–15]. Combination of both the two ways is performed for a good rate capability, i.e., embedding $LiFePO_4$ nanoparticles in a carbon matrix [9]. Usually, the $LiFePO_4$ nanoparticles can be prepared via a solid-state reaction or a sol–gel process, but both methods contain a complicated procedure and a longtime sintering process. In addition, the obtained spherical nanoparticles have too large surface area and thus a quite low tap density, which is not welcome for industrial processing, transport and storage. And the complicated procedure for the high-temperature reactions directly gives difficulties of stable commercial production of $LiFePO_4$, which is also one of the biggest obstacles for the wide application of $LiFePO_4$ at

H. Xiang · H. Wang (✉)
School of Chemistry & Chemical Engineering, South China University of Technology, Guangzhou 510640, Guangdong, China
e-mail: hhwang@scut.edu.cn

H. Xiang · J. Wu (✉)
Department of Chemistry, National University of Singapore, 3 Science Drive 3, 117543 Singapore, Singapore
e-mail: chmwuj@nus.edu.sg

D. Zhang · Y. Jin · C. Chen
Department of Materials Science and Engineering, University of Science and Technology of China, Hefei 230026, Anhui, China

present. Thus, it is vitally significant to prepare the pure $LiFePO_4$ with a suitable size or morphology via a simple route. Whittingham reported that well-crystalline $LiFePO_4$ platelets could be prepared quite quickly in a low-temperature hydrothermal process [16]. The plate-like crystals had large facets in the ac-plane, i.e., (020) plane and regulable thickness from several hundred nanometers to 2 μm in the *b*-axis of the olivine structure [17, 18]. It has been reported that Li ion diffusion in the $LiFePO_4$ crystal carries out along the b-axis and charge transfer occurs in the ac-plane of the crystalline surface [19–22]. Since Li ion only predominantly transfer along the one-dimensional channels composed of the FeO_6 octahedra and PO_4 tetrahedra, it is desirable to surmise that the $LiFePO_4$ platelets with a thickness of *c* value has the similar Li ion diffusion distance with the $LiFePO_4$ powders with the size of c value, as illustrated in Fig. 1. The common drawbacks from the nanoparticles mentioned above could be effectively overcome by this plate-like candidate prepared by a hydrothermal synthesis. Moreover, hydrothermal synthesis of $LiFePO_4$ also has the advantages of low cost of precursors, low-energy cost, and comparatively short reaction times. So the hydrothermal synthesis of $LiFePO_4$ is very promising for the development of large-scale Li-ion batteries. In fact, commercial production of $LiFePO_4$ by the hydrothermal synthesis now is under way.

The hydrothermal synthesis of $LiFePO_4$ has been investigated by many groups. Whittingham and coworkers were the first to report the hydrothermal synthesis of $LiFePO_4$ [16, 23–25]. They found that the temperature for hydrothermal reaction had significant effects on the iron disorder onto the lithium sites, which could be eliminated by using a reaction temperature above 175 °C. The introduction of a soluble reductant, such as sugar or ascorbic acid, in the hydrothermal reaction was effective to minimize the oxidation of the ferrous to the ferric. Dokko and coworkers declared that a heat treatment after the hydrothermal synthesis of $LiFePO_4$ for a short time (only 30 min) was very helpful for crystallizing the amorphous layer on the outmost surface of the as-synthesized particles, which achieved a higher capacity [26–28]. They also investigated the effect of pH of the precursor solution on the particle morphology, crystal orientation, and electrochemical reactivity of the prepared $LiFePO_4$ particles [17]. The plate-like $LiFePO_4$ crystals were easily obtained from weak acidic solutions of $4 < pH < 6.5$. The plate-like crystal with a large facet in the ac-plane exhibited the highest electrochemical reactivity among all the samples with various morphologies [18]. As mentioned above, it is very significant to prepare the well-crystalline $LiFePO_4$ plate-like with a very thin thickness. It has been proved that the particle size of $LiFePO_4$ decreases with increasing concentration of starting materials in the precursor solution, due to the more nuclei provided for the crystal growth in the solution with higher concentration [14]. But to our best knowledge, in a solution with too high concentration there is no enough space for the regular crystal growth on the nuclei. In the presence of some surfactant or chelating agent, such as hexadecyltrimethylammonium bromide (CTAB), phenanthroline or nitrilotriacetic acid, the obtained samples were not plate-like, although the fine $LiFePO_4$ with pure phase could be prepared with sphere-like or nanowire [29–32]. Tajimi et al. [33] reported that the addition of polyethylene glycol (PEG400) to the precursor solution was effective to reduce the particle size. So far, few reports have been investigated the effect of a co-solvent on the hydrothermal

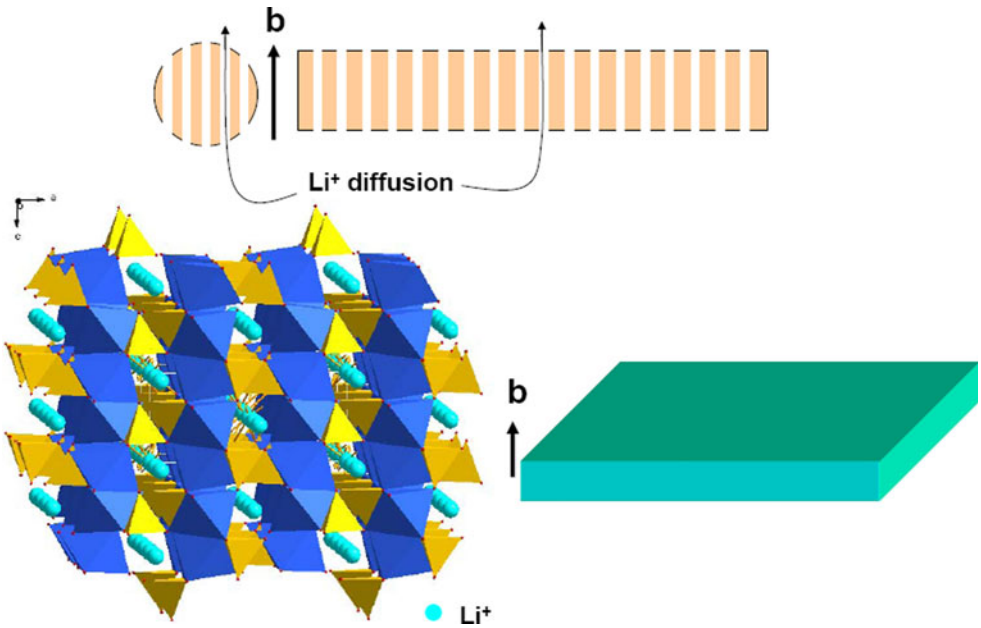

Fig. 1 Crystal structure of olivine $LiFePO_4$ and illustration of the one-dimensional diffusion channels for Li^+ ions in the sphere-like and plate-like materials

synthesis of $LiFePO_4$. Herein, for the first time, a polyol compound, tetraethylene glycol (TEG) was introduced into the hydrothermal reaction system as co-solvent in order to reduce the size of the products but not change the plate-like morphology. Finally ultra-thin $LiFePO_4$ platelets were prepared successfully and investigated as cathodes in the Li-ion batteries.

Experimental

$LiFePO_4$ was synthesized by a modified hydrothermal route as follows: $FeSO_4{\cdot}7H_2O$ (15 mmol) and H_3PO_4 (15 mmol) as the starting materials were added into the 50 ml deionized water, and a light green solution was formed. After 0.1 g ascorbic acid was introduced as an in situ reducing agent to minimize the oxidation of ferrous to ferric, the color of the solution changed to brown. LiOH (45 mmol) was dispersed in 200-ml TEG with stirring. Then the LiOH suspension was slowly dropped into the aqueous solution with vigorous stirring. A viscous and light blue suspension was obtained and subsequently transferred into a 280 ml capacity Teflon-lined stainless steel autoclave. The autoclave was sealed and heated at 190 °C for 5 h, followed by being cooled down to room temperature naturally. Precipitates were collected by suction filtration and washed with deionized water and acetone. After dried at 80 °C for 1 h in the vacuum oven, light green powder was collected and then heated at 500 °C for 1 h in nitrogen atmosphere. The obtained $LiFePO_4$ powder was gray. $LiFePO_4$/C composite was also prepared by firing $LiFePO_4$ with glucose ($LiFePO_4$:glucose = 1:0.15, w/w) at 600 °C for 2 h in nitrogen atmosphere, usually along with less than 5% carbon residue. For comparison, other two $LiFePO_4$ samples were prepared by a similar route just without TEG introduced. One (denoted as *o*-$LiFePO_4$) was prepared in 50 ml H_2O (without TEG), but the other (denoted as *t*-$LiFePO_4$) was prepared in 250 ml H_2O, where 200 ml TEG was replaced by H_2O with the same volume.

The X-ray diffraction (XRD) measurement was carried out on a Bruker D8 Advance X-ray diffraction using a Cu Kα radiation source ($\lambda = 1.5406$ Å). The diffraction data were collected for 6 s at each 0.02° step width over a 2θ range from 10° to 70°. Scanning electron microscope (SEM) measurements were carried out on a field emission scanning electron microscope (JEOL-6300F) at 5 kV.

The electrochemical performance of as-prepared $LiFePO_4$ was investigated using coin cells (CR2032) assembled in an argon-filled glove box (Mikrouna, super 1220). Composite electrodes consisting of $LiFePO_4$ or $LiFePO_4$/C composite (70 wt%), Super P carbon black (20 wt%) and poly(vinylidene fluoride) (PVDF) (10 wt%) were made by a tape-casting process on aluminum foils. The mass loading was about 2.5 mg cm^{-2}. Celgard 2400 microporous polypropylene membrane was used as separator. The electrolyte consisted of a solution of 1 M $LiPF_6$ in ethylene carbonate (EC)/diethyl carbonate (DEC) (1:1 w/w). Lithium foil was used as counter electrode. The assembled cells were galvanostatically cycled between 2.4 and 4.3 V at different current rates on a multi-channel battery cycler (Neware BTS2300, Shenzhen). Herein, a cycling rate of nC means that it takes $1/n$ h for the cell to drain in a predefined voltage window. Cyclic voltammograms (CV) were performed using the coin-cells over the potential range of 2.4–4.3 V at a scanning rate of 0.2 mV s^{-1} on a Zahner IM6ex Electrochemical Workstation.

Results and discussion

Figure 2 shows the XRD results of pure $LiFePO_4$ and $LiFePO_4$/C composite materials. Both samples exhibit single phase of $LiFePO_4$ with an ordered olivine structure indexed with the orthorhombic Pnma space group (No. 62), without any other impurity phase detected. The narrow diffraction peaks indicate that both samples are highly crystalline. Here, we find that the inert atmosphere (N_2 or Ar) is not necessary for preparing the highly pure $LiFePO_4$ crystal in the hydrothermal synthesis when some reductant (ascorbic acid, citric acid, or something else) is used. However, it must be noted that too much additive, either reductant (i.e., ascorbic acid, citric acid) or surfactant (i.e., CTAB), may have a remarkable effect on the pH value of the reaction system, which is a key parameter for the hydrothermal synthesis of $LiFePO_4$.

The morphology for $LiFePO_4$ particles is shown in Fig. 3, together with the image of $LiFePO_4$/C composite. The obtained $LiFePO_4$ powder is composed of agglomerated platelets (Fig. 3a). It seems that the $LiFePO_4$ nanoparticles with high surface energy tend to form many

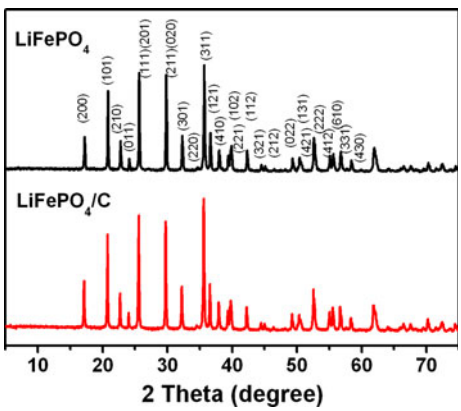

Fig. 2 XRD patterns of $LiFePO_4$ and $LiFePO_4$/C prepared via the hydrothermal reaction

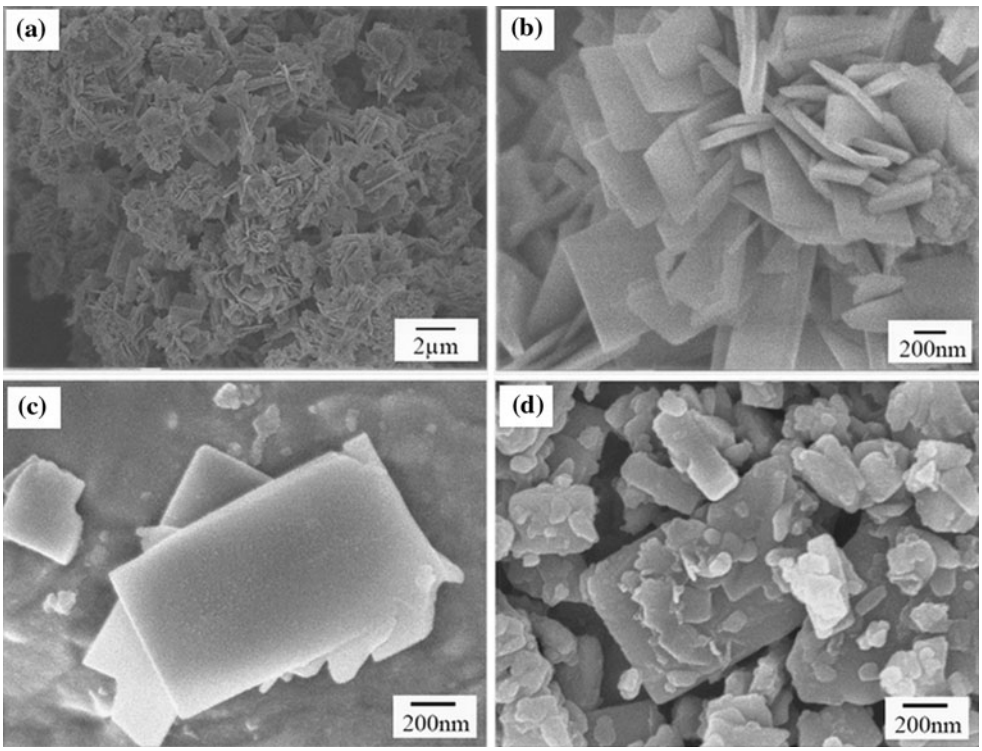

Fig. 3 SEM images of $LiFePO_4$ (**a**–**c**) and $LiFePO_4$/C composite (**d**)

clusters under the hydrothermal conditions, which can also be easily found in the previous literatures [17, 33]. From Fig. 3b and c, the $LiFePO_4$ platelets have typically an ultra-thin thickness of 50–80 nm, and the platelets are rectangles with the size of about 400 × 700 nm^2. For the $LiFePO_4$/C composite, the morphology of the original $LiFePO_4$ keeps intact basically and most carbon particles are attached on the surface of the $LiFePO_4$ platelets, just as shown in Fig. 3d. The effect of TEG on the hydrothermal preparation process of $LiFePO_4$ is investigated by comparing the morphologies of the samples prepared with or without TEG. Figure 4 shows that *o*-$LiFePO_4$ and *t*-$LiFePO_4$ prepared without TEG have the thickness of about 0.5 and 1–2 μm, respectively, and both the samples are rhombic, which are similar as the previous literature [16, 18]. The fine structure of ultra-thin $LiFePO_4$ platelets is probably attributed to the introduction of TEG in the hydrothermal process. Usually, the added LiOH can react with the acidic solution containing Fe^{2+} and PO_4^{3-} to form $LiFePO_4$ nuclei. Subsequently, these nuclei grow and become larger and larger by the Ostwald ripening process. According to the previous reports, the final shape is determined by the different growth rate of different faces on the nuclei, which are associated with surface energies of the corresponding faces [34]. The surface energy of the (010) layers is much smaller than that of the next face in most hydrothermal reaction systems [35]. So the particle growth tends to form the crystal with large (010) face. Consequently, the product with plate-like shape is formed with a small size in the [010] direction [18, 34]. In our system, the starting materials, i.e., lithium salt and iron salt can easily dissolve in the water, but nearly insoluble in the TEG. However, the TEG molecules dissolved not only have a strong chelating interaction with the metal ions in the aqueous solution, but also work as a co-solvent with high viscosity. Therefore, the slowed rate of mass transfer naturally results in the limited crystal growth. On the other way, the introduction of plenty of TEG (three times more than water by weight) can separate the nuclei in the farer distance, which can also slow down the rate of the Ostwald ripening process. In addition, TEG can also play a role of surfactant, which could reduce the attachment energy on the (010) surface of the nuclei. All the effects of TEG result in the formation of the ultra-thin $LiFePO_4$ platelets.

Figure 5 shows the cyclic voltammetry results of the $LiFePO_4$ and $LiFePO_4$/C composite materials in the coin-cells during the first three cycles. Both the materials have the anodic peak at 3.6 V and the cathodic peak at 3.3 V, which are correlated to the lithium extraction and insertion from the olivine structure, respectively. For the bare $LiFePO_4$, the symmetrical redox peaks look quite broad, which suggests that there is a notable polarization. After the carbon coating, the $LiFePO_4$/C composite is endowed with quite narrow and sharp redox peaks, along with the

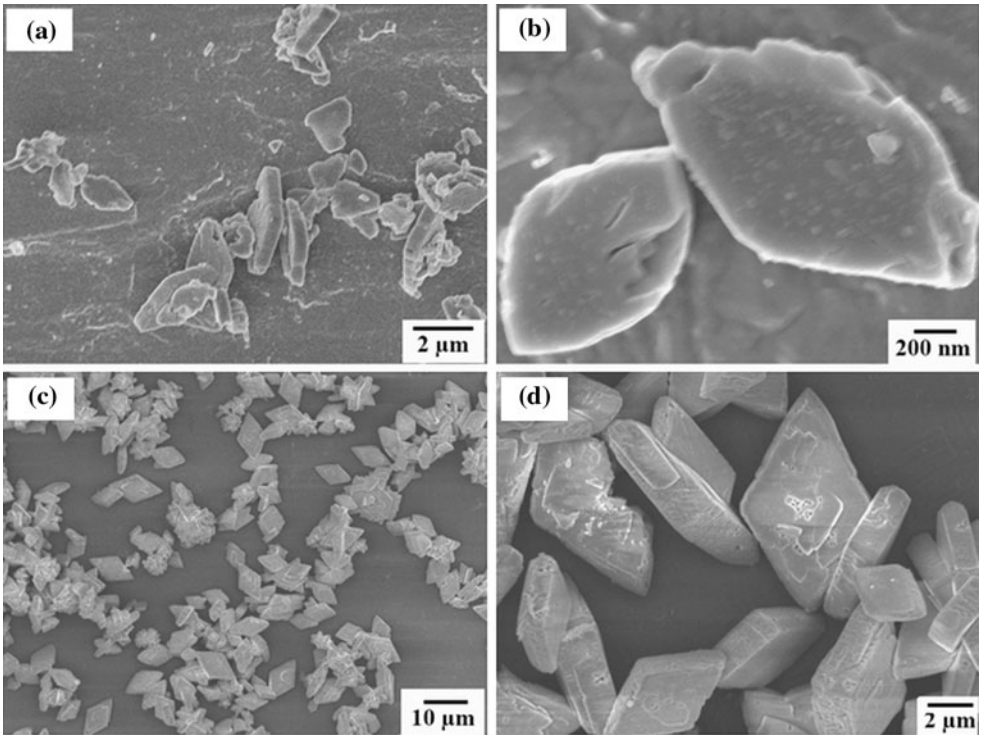

Fig. 4 SEM images of o-$LiFePO_4$ (**a**, **b**) and t-$LiFePO_4$ (**c**, **d**) prepared without TEG

increased peak current. It is the result of the enhanced electrochemical activity of the $LiFePO_4$/C composite. It is strongly indicated that the electronic conductivity of the ultra-thin $LiFePO_4$ platelets should also be improved by the surface coating technology for the fast charge transfer on the surface, although they have the very short diffusion distance for the Li ions.

The voltage profiles of the first three cycles and cycling performance of $LiFePO_4$ and $LiFePO_4$/C composite materials in the corresponding cells are shown in Fig. 6. The initial discharge capacity of $LiFePO_4$ is 137 mAh g^{-1} with a high coulombic efficiency of 98% (Fig. 6a). Both the discharge capacity and coulombic efficiency keep a high level in the sequent cycles. For the $LiFePO_4$/C composite, the discharge capacity is slightly improved to 140 mAh g^{-1} because of the enhanced electronic conductivity. But the coulombic efficiency is not as high as that of the pristine $LiFePO_4$. We suppose that the possible reason for the reduced coulombic efficiency could be the loss of some Li ions extracted from the $LiFePO_4$ crystal lattice during the charging process due to the Li absorption in the coated carbon layer. In addition, it is obvious that the plateau gap between the charge and discharge voltage profiles becomes small after carbon coating, which also indicates that the polarization is decreased obviously. Figure 6b shows the cycling performance of $LiFePO_4$ and $LiFePO_4$/C composite electrode. Here the electrode was charged up to 4.3 V at

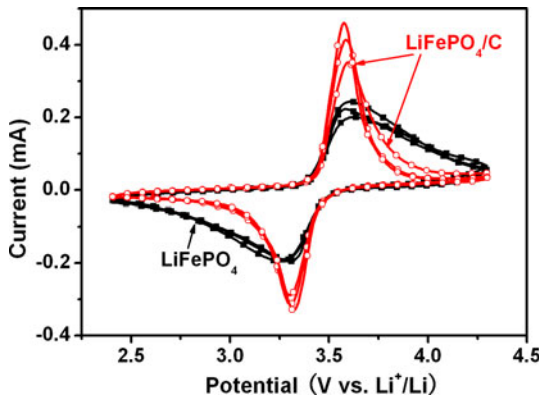

Fig. 5 Cyclic voltammograms of $LiFePO_4$ and $LiFePO_4$/C. The scan rate is 0.2 mV s^{-1}

0.2 C and discharged at 0.2, 0.5, 1 C, respectively. At 0.2 C, the discharge capacity of $LiFePO_4$/C is only slightly higher than that of $LiFePO_4$ (137 mAh g^{-1}). At 0.5 and 1 C, the $LiFePO_4$/C composite has not shown obvious capacity loss, and also exhibited excellent cycling performance. However, at 0.5 C, the discharge capacity of bare $LiFePO_4$ is about 115 mAh g^{-1}, and only 94 mAh g^{-1} can be released at the discharge rate of 1 C, which means that the ultra-thin $LiFePO_4$ can still fail to exhibit a satisfying rate capability, due to its poor electronic conductivity. Surface coating technology to enhance the electronic conductivity of $LiFePO_4$ seems to be necessary to make it applicable in the

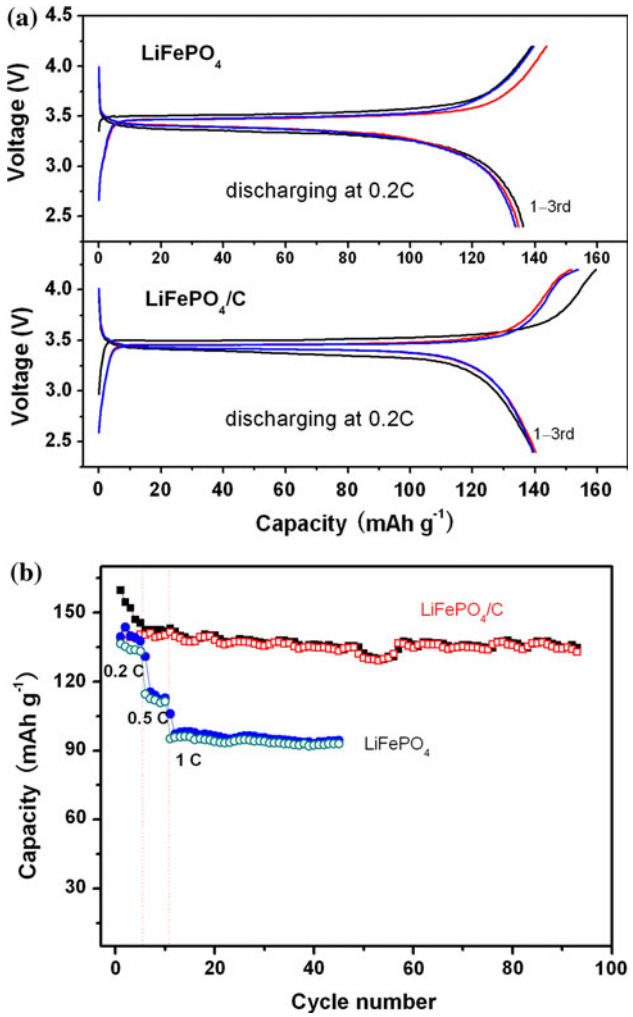

Fig. 6 The initial voltage profiles (**a**) and cycling performance (**b**) of the $LiFePO_4$ and $LiFePO_4$/C. All the cells are charged at a rate of 0.2 C

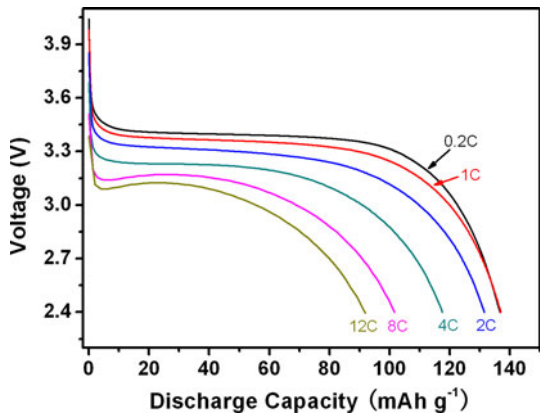

Fig. 7 Discharge curves of $LiFePO_4$/C composite cathode at 0.2–12 C rates. The electrode was charged up to 4.3 V at 0.2 C prior to each discharge and discharged at various rates

lithium power batteries. The rate capability of $LiFePO_4$/C is further investigated. Figure 7 shows the discharge voltage profile at the 0.2–12 C rates. There seems to be no obvious difference between the 0.2 and 1 °C, except for the slightly depressed voltage plateau at 1 C. At 2 C, the discharge capacity decreases distinctly from the 140 mAh g^{-1} at 1 C to 136 mAh g^{-1}, along with the voltage plateau dropping to 3.3 V. At 4 and 8 C, the discharge capacities are 120 and 104 mAh g^{-1}, respectively. Even at 12 C, corresponding to a discharge time of about 5 min, the cell can still release a quite high capacity of about 95 mAh g^{-1}. Moreover, the voltage plateau of over 60% capacity is above 3.0 V, which indicates that the ultra-thin $LiFePO_4$ platelets are promising cathode material for the batteries with not only high power density but also high energy density.

Conclusions

The requirement for the development of large-scale Li-ion batteries is the safe and stable materials with high energy density and power density. The ultra-thin $LiFePO_4$ platelets with about 50–80 nm thickness, as an intrinsically safe cathode material, have an advantage of tap density and comparable diffusion kinetics for Li ion over common spherical nanoparticles. It was demonstrated that this cathode material exhibited quite high reversible capacity, i.e., 137 mAh g^{-1} at 0.2 C. After carbon coating, the obtained $LiFePO_4$/C composite cathode had the enhanced electronic conductivity, and thus the rate capability had been improved significantly. At 8 and 12 C, the composite had the discharge capacity of 104 and 95 mAh g^{-1}, respectively. All the results show that the ultra-thin $LiFePO_4$ platelets and its composite are very promising for the application in the large-scale Li-ion batteries.

Acknowledgements This study was supported by National Science Foundation of China (grant No. 21006033 and 20703013) and the Fundamental Research Funds for the Central Universities, SCUT (2009220038). We are also grateful to A*Star SERC Thematic Strategic Research Programme—Sustainable Materials: Composites & Lightweights (R-143-000-401-305).

References

1. Yamada A, Koizumi H, Nishimura SI, Sonoyama N, Kanno R, Yonemura M, Nakamura T, Kobayashi Y (2006) Nat Mater 5:357
2. Scrosati B, Garche J (2010) J Power Sources 195:2419
3. Tollefson J (2008) Nature 456:436
4. Padhi AK, Nanjundaswamy KS, Goodenough JB (1997) J Electrochem Soc 144:1188
5. Yamada A, Chung SC, Hinokuma K (2001) J Electrochem Soc 148:A224
6. Li ZH, Zhang DM, Yang FX (2009) J Mater Sci 44:2435. doi: 10.1007/s10853-009-3316-z

7. Anderesson AS, Thomas JO (2001) J Power Sources 97(98):498
8. Ravet N, Chouinard Y, Magnan JF, Besner S, Gauthier M, Armand M (2001) J Power Sources 97:503
9. Wu XL, Jiang LY, Cao FF, Guo YG, Wan LJ (2009) Adv Mater 21:2710
10. Wang Y, Wang J, Yang J, Nuli Y (2006) Adv Funct Mater 16:2135
11. Crose F, Epifanio AD, Hassoun J, Deptula A, Olczac T, Scrosati B (2002) Electrochem Solid State Lett 5:A47
12. Park KS, Schougaard SB, Goodenough JB (2007) Adv Mater 19:848
13. Franger S, Le Cras F, Bourbon C, Rouault H (2003) J Power Sources 119(121):252
14. Ellis B, Wang HK, Makahnouk WRM, Nazar LF (2007) J Mater Chem 17:3248
15. Chung SY, Bloking JT, Chiang YM (2002) Nat Mater 1:123
16. Yang S, Zavalij PY, Whittingham MS (2001) Electrochem Commun 3:505
17. Dokko K, Koizumi S, Nakano H, Kanamura K (2007) J Mater Chem 17:4803
18. Kanamura K, Koizumi K, Dokko K (2008) J Mater Sci 43:2138. doi:10.1007/s10853-007-2011-1
19. Morgan D, Van der Ven A, Ceder G (2004) Electrochem Solid State Lett 7:A30
20. Chen G, Song X, Richardson T (2006) Electrochem Solid State Lett 9:A295
21. Saravanan K, Vittal JJ, Reddy MV, Chowdari BVR, Balaya P (2010) J Solid State Electrochem 14:1755
22. Li LX, Tang XC, Liu HT, Qu Y, Lu ZG (2010) Electrochim Acta 56:995
23. Chen J, Whittingham MS (2006) Electrochem Commun 8:855
24. Chen J, Wang S, Whittingham MS (2007) J Power Sources 174:442
25. Chen J, Vacchio MJ, Wang S, Chernova N, Zavalij PY, Whittingham MS (2008) Solid State Ion 178:1676
26. Dokko K, Koizumi S, Sharaishi K, Kanamura K (2007) J Power Sources 165:656
27. Shiraishi K, Dokko K, Kanamura K (2005) J Power Sources 146:555
28. Nakano H, Dokko K, Koizumi S, Tannai H, Kanamura K (2008) J Electrochem Soc 155:A909
29. Meligrana G, Gerbaldi C, Tuel A, Bodoardo S, Penazzi N (2006) J Power Sources 160:516
30. Wang ZL, Su SR, Yu CY, Chen Y, Xia DG (2008) J Power Sources 184:633
31. Wang GX, Shen XP, Yao J (2009) J Power Sources 189:543
32. Ferrari S, Lavall RL, Capsoni D, Quartarone E, Magistris A, Mustarelli P, Canton P (2010) J Phys Chem C 114:12598
33. Tajimi S, Ikeda Y, Uematsu K, Toda K, Sato M (2004) Solid State Ion 175:287
34. Fisher CAJ, Islam MS (2008) J Mater Chem 18:1209
35. Qin X, Wang XH, Xiang HM, Xie J, Li JJ, Zhou YC (2010) J Phys Chem C 114:16806